NASA Technical Paper 3214

July 1992

Development of a Truss Joint for Robotic Assembly of Space Structures

George F. Parma

NASA

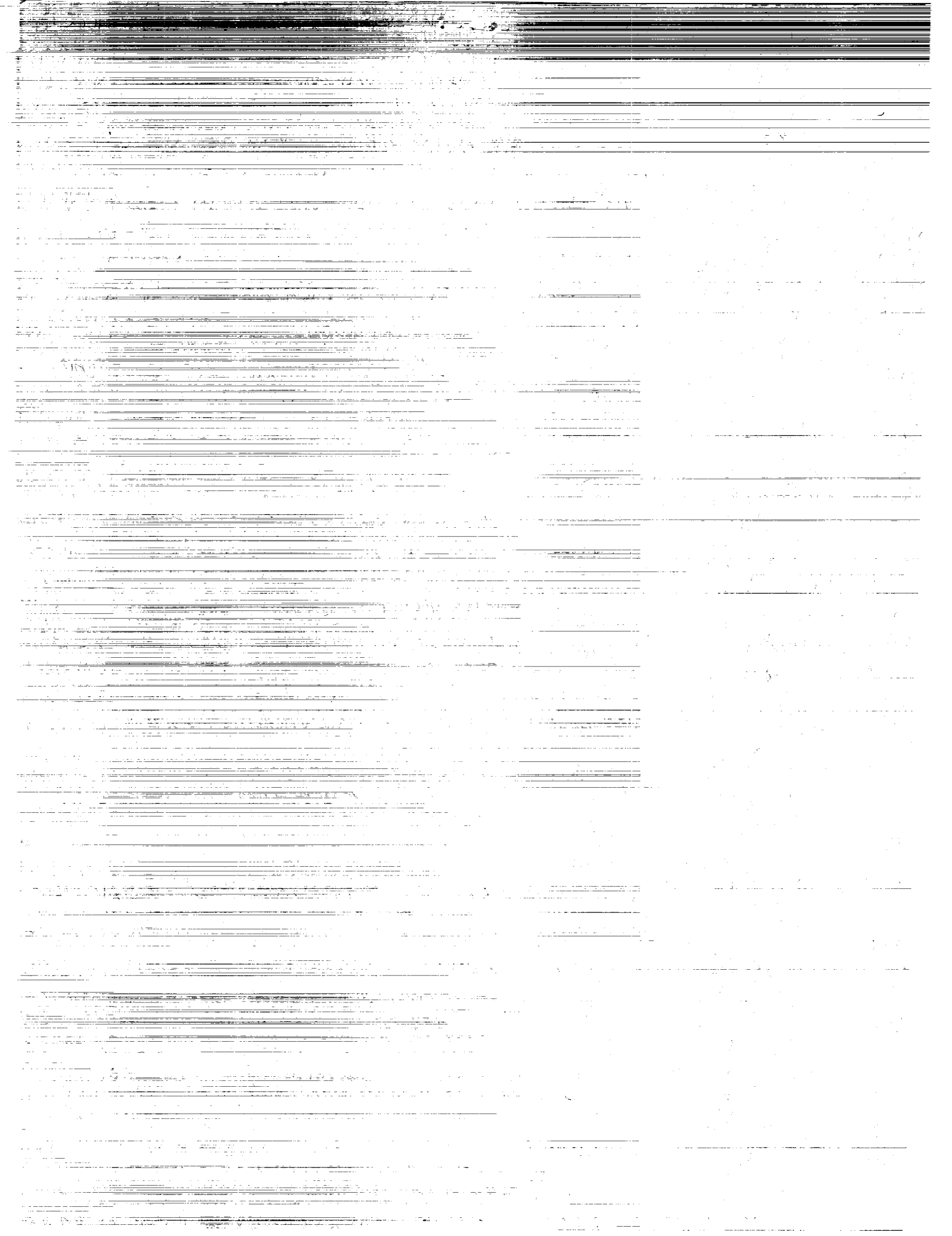

NASA Technical Paper 3214

1992

Development of a Truss Joint for Robotic Assembly of Space Structures

George F. Parma
Lyndon B. Johnson Space Center
Houston, Texas

National Aeronautics and Space Administration

Office of Management

Scientific and Technical Information Program

Contents

Tables

Figures

Acronyms

ACCESS	Assembly Concept for Construction of Erectable Space Structure
ARASS	Automated Robotic Assembly of Space Station
ASSAP	Automated Space Servicing and Assembly Platform
ATAD	ACESS Telerobotic Assembly Demonstration
BAT	Beam Assembly Teleoperator
DFA	Design for Assembly
EASE	Experimental Assembly of Structures in EVA
EVA	Extravehicular Activity
JSC	Johnson Space Center
LTM	Laboratory Teleoperator Manipulator
LVDT	Linear Voltage Differential Transformer
RAMS	Robotics and Mechanical Systems
RMS	Remote Manipulator System
WETF	Weightless Environment Training Facility
WIS	Workcell Integration System

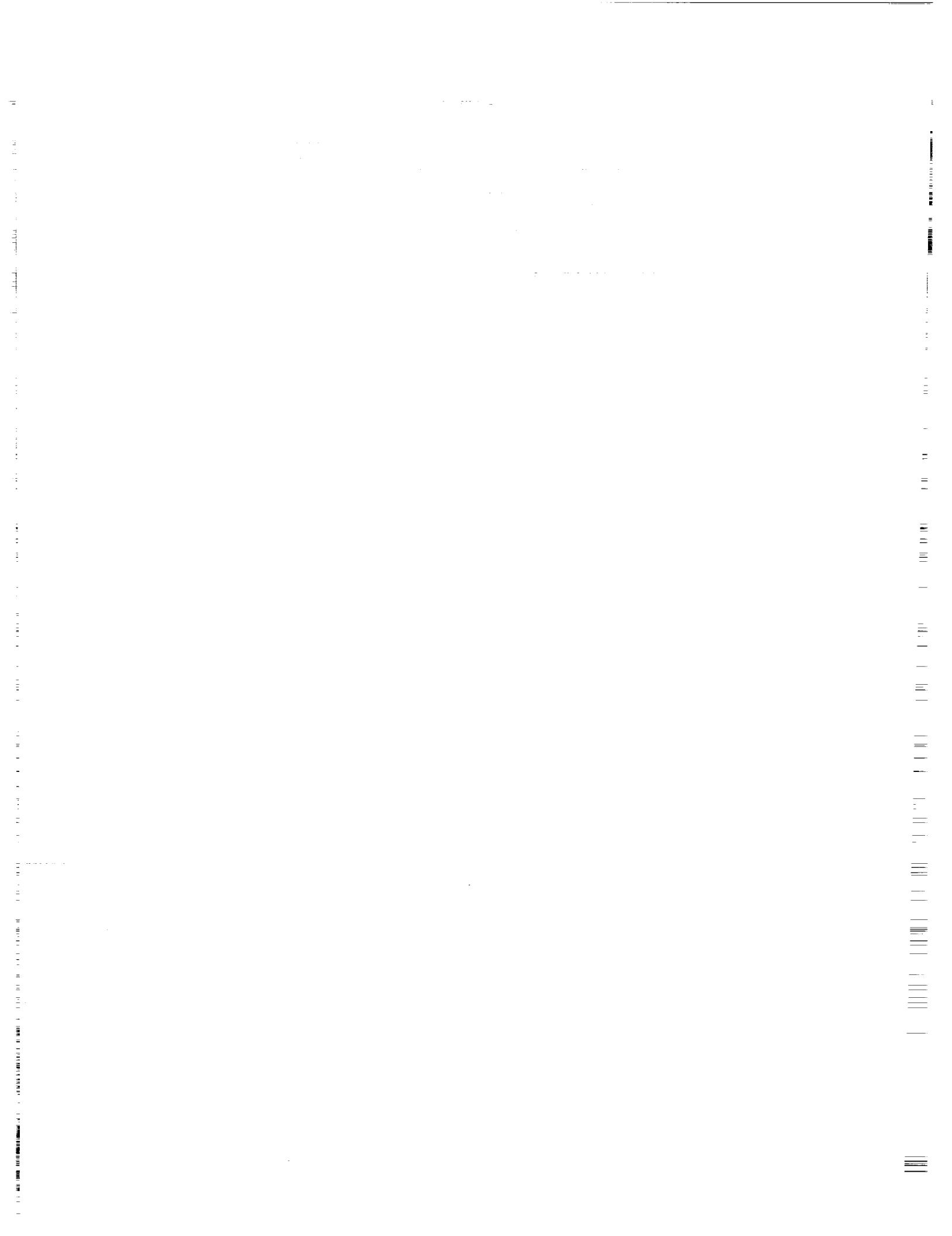

Introduction

This report presents the results of a study undertaken to quantify the advantages of designing a structural fastener for ease of robotic assembly—a concept we will refer to as "robot-friendly." The study was conducted by the Robotics and Mechanical Systems (RAMS) Laboratory in the Structures & Mechanics Division at the NASA-Johnson Space Center (JSC) in 1990. Four prototype robot-friendly structural joints were designed, built, and evaluated for use in a full-scale test called the Automated Robotic Assembly of Space Station (ARASS) demonstration. The joints were tested for ease of robotic assembly as well as for structural properties, and the best joint was chosen for use in the demonstration.

The author would like to acknowledge the contributions to this team effort made by all the members of the RAMS Laboratory. Particular thanks belong to Erik Evenson, Steve Ruiz, Lebarian Stokes, John Thompson, and Mark Vandeberghe.

Identification of commercial products in this report is used to describe the test facility and does not constitute official endorsement, expressed or implied, of such products by the National Aeronautics and Space Administration.

Space-Based Assembly

Until now, the U.S. space program has relied upon launching space vehicles as completely assembled and integrated systems. As we look to future programs, the sizes of the vehicles necessary become prohibitively large to launch as complete assemblies. The next logical step is to launch the vehicle in pieces and assemble it on orbit or on another celestial body; such vehicles can usually be lighter, more efficient structures because they do not have to withstand launch and landing loads in their as-assembled configurations. Assembly and maintenance of many of these structures will be best accomplished by astronauts conducting extravehicular activity (EVA) or by robotic devices. We will presently consider these two methods.

EVA Structural Assembly

The subject of EVA assembly has been under study by NASA for at least 15 years. In that time, numerous evaluations have been performed in neutral buoyancy simulators, like the Weightless Environment Training Facility (WETF) at JSC, and in numerous other water tanks throughout the country. These simulations have used successively higher and higher fidelity mockups to prove the concept of EVA structural assembly and investigate the problems associated with it. Flight experiments to demonstrate on-orbit EVA construction techniques first flew on STS-61B in December 1985—these were the Experimental Assembly of Structures in EVA (EASE) and the Assembly Concept for Construction of Erectable Space Structure (ACCESS). Results from many of these tests are summarized in [1].

Numerous mock-ups of the 5-meter (16.4-ft.) space station truss have been assembled in neutral buoyancy simulators since that time. The crew comments have mainly been related to positioning and reach from assembly work platforms, hand fatigue from multiple joint actuations, difficulties in handling and distinguishing between longeron and diagonal struts, glove wear, difficulties in achieving a connection due to joint intolerance to misalignment, and the need for visual cues to confirm the state of the connector [2,3,4]. It is a repetitive and labor-intensive task, but quite doable.

Robotic Structural Assembly

A limited number of ground-based robotic structural assembly demonstrations have been conducted. Most of these evaluations have been conducted under teleoperator control with EVA hardware. For example, the Beam Assembly Teleoperator (BAT) at the Massachusetts Institute of Technology was used to assemble the EASE truss, and the Laboratory Teleoperator Manipulator (LTM) was used to assemble ACCESS (in conjunction with a human assistant) at Oak Ridge National Laboratory.

The RAMS lab has also studied telerobotic assembly with the ACCESS Telerobotic Assembly Demonstration (ATAD). This demonstration was performed in the JSC structures laboratory using WETF ACCESS hardware and a teleoperated hydraulic manipulator. This hardware had been optimized for gloved EVA assembly, and that led to numerous difficulties for teleoperation. The joints were difficult to align because of their tight tolerances, often tripped shut unintentionally (and were impossible to reset), and were difficult to visually align and verify [5].

But structural assembly is repetitious, well structured, and labor intensive; it is therefore well suited for complete automation. Very few groups have studied automated structural assembly. Apart from our colleagues at NASA's Langley Research Center [6], no other groups have extensively studied this technique. This was the impetus for inception of the ARASS demonstration.

The ARASS Demonstration

The ARASS demonstration was conceived to establish general confidence in robotics as a *tool* to accomplish *meaningful* tasks. It will do so by demonstrating the assembly of two bays of full scale 5-meter box truss in a totally automated robotic workcell as shown in figure 1. This workcell configuration is representative of one which could be used to build 5-meter truss out of the Space Shuttle Orbiter payload bay in low Earth orbit. We have had to design heavy tower structures to offset the pull of gravity, but an actual flight system might use something like the Shuttle's remote manipulator system (RMS) instead.

The ARASS demonstration is a ground-based test which will utilize two 7-degree-of-freedom Robotics Research K-1607 manipulators, each outfitted with a specialized end effector, force/torque sensor, and machine vision system. Each robot is mounted on a large 2-degree-of-freedom platform, and the two of these together are called the Automated Space Servicing and Assembly Platform (ASSAP). The ASSAP is a general purpose system which will allow the robots to translate 4.6 meters (15.1 ft.) vertically and 7.8 meters (25.7 ft.) horizontally on either side of the truss. The entire assembly process will take place autonomously, with all the devices being controlled by a central workcell control program called the Workcell Integration System (WIS). WIS is being developed and implemented by the RAMS lab.

The Robot-Friendly Structural Joint Study

The key element to the success of the ARASS demonstration is the use of hardware that is easy for robots to assemble, or "robot-friendly." This means that the hardware incorporates many of the principles generally associated with design for assembly (DFA); e.g., simple insertion operations, generous lead-in chamfers, and self-aligning parts. Discussions on the principles of DFA may be found in [7], [8] and many other sources. There are additional advantages to be gained by designing specifically with automation in mind. In fact, in most cases in industry where cost comparisons are made in order to show the supposed benefits of automatic assembly, careful study usually shows that the benefits have been obtained through redesigning the product for assembly rather than through assembly automation [8]. By designing with robotic assembly in mind, we expect to create a joint which is easier for either an astronaut *or* a robotic device to put together.

Fig. 1 ARASS Workcell Configuration

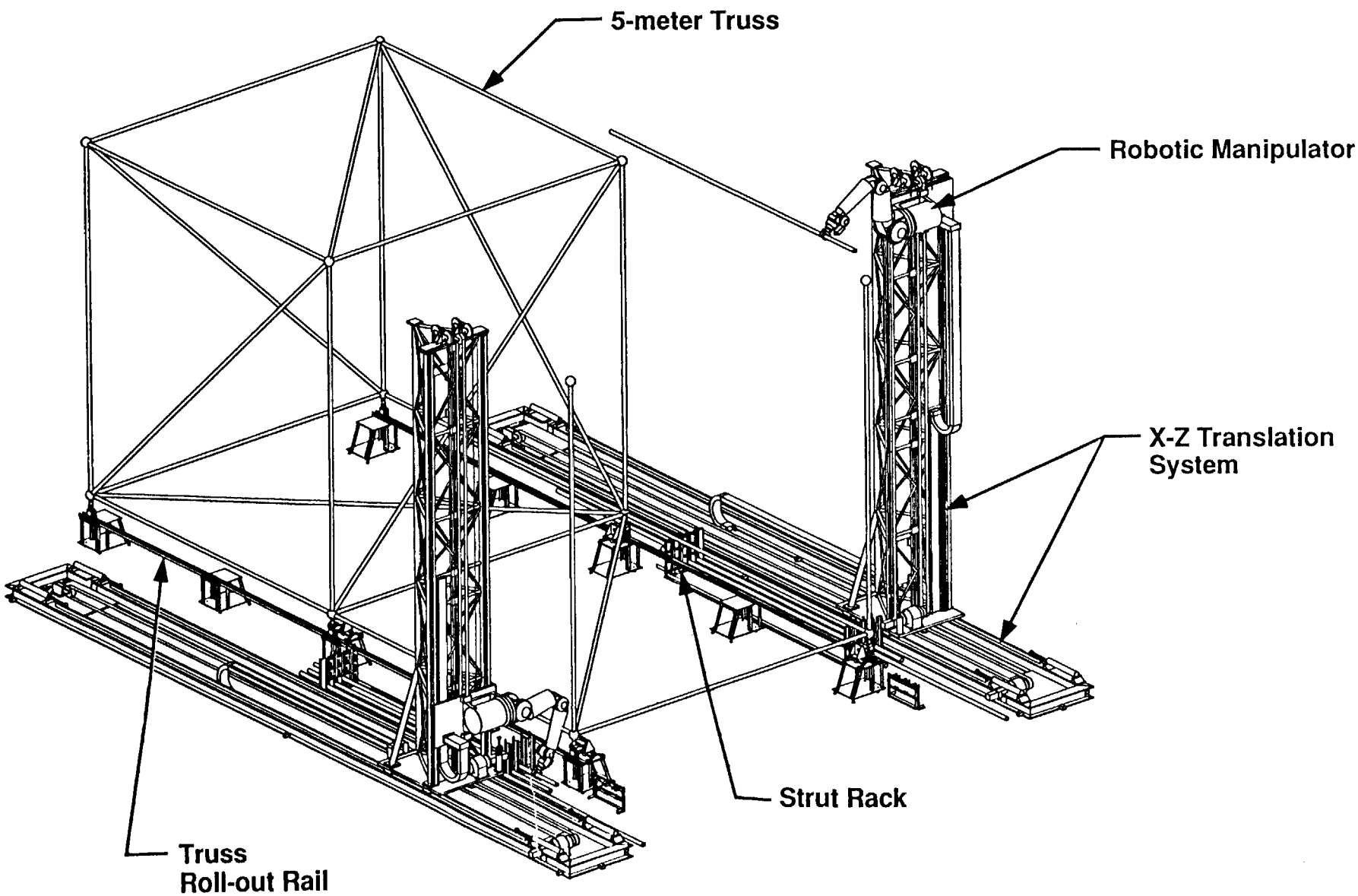

The objective of this study was to start with a clean slate and design a truss joint to accommodate both automated and EVA assembly while taking maximum advantage of the robotic assembly tool. The result would be a truss structure with all the advantages of tooled assembly plus easier EVA assembly.

This was the study procedure:

1. Develop design requirements consistent with the current space station truss design while meeting the requirements of the ARASS demonstration.
2. Design and build prototype hardware to meet those requirements.
3. Test prototypes for ease of robotic assembly.
4. Test prototypes for structural properties.
5. Analyze test data.
6. Choose the best overall joint/end effector system; incorporate the best features of all joints into a final design to be manufactured for the full-scale ARASS demonstration.

Designing for Robotic Assembly

The current state-of-the-art truss joints for on-orbit space structural assembly were designed specifically for EVA hand assembly (as discussed earlier). The design of these fasteners focused on the ease with which a gloved astronaut could assemble hundreds of these joints without excessive fatigue or glove wear.

These requirements forced a compromise for simplicity of operation at the price of weight, complexity, and cost. Each joint has its own internal mechanism *plus* an external mechanism (e.g., a lever or collar) which adapts the connector to the gloved astronaut's hand (one might think of this as incorporating the tool necessary to tighten the joint into every single unit). The designs also assume that whatever motions the astronaut does to operate the joint, a robot could be made to do as well. As it turns out, the robot must perform extremely difficult motions to duplicate these operations, and/or the gripper must incorporate an *additional* mechanism which allows it to mimic the motions of the gloved astronaut. This duplication results in an overall system which is twice as complex as is necessary.

Another drawback shared by these EVA truss joints is that they are very intolerant of misalignments. They assume that the person performing the assembly will provide the compliance and exhibit the dexterity necessary to overcome such problems. Robots are, in general, not as adaptive to such conditions. This can result in the task becoming difficult or impossible to accomplish. Even if the robot were able to compensate for such deficiencies, it still operates on a perfect model of the world, and assumes its own actions are perfect. Many errors in the system are still unaccounted for, such as gripper misalignment, deflection in the manipulator structure, inaccuracies in the robot drive system, and inaccuracies in the jig which holds the truss during assembly. Fasteners which are not designed to accommodate such misalignments are therefore unsuitable for automated assembly.

Another advantage of designing a joint for robotic assembly is increased system efficiency. Since we are designing the robotic end effector and the truss joint as a system, we can optimize the end-effector-to-joint interface to achieve the most efficiency. We can also place as much of the complication as possible in the end effector (of which we are building only two), and make the truss joint (of which we may be building hundreds or thousands) much simpler, stiffer, lighter, and less expensive than its EVA counterpart.

Design Requirements

Considerable discussion went into the formulation of the design guidelines for this fastener. These requirements (outlined in table 1) were developed based on our best assessment of the space station truss requirements at the time.

A comment should be made here about the "soft capture" requirement (the eighth requirement listed in table 1). A "soft capture" device is a mechanism which loosely connects a joint such that a person can let go of the joint without it coming apart. "Soft capture" has always been a requirement for EVA joints as echoed by [1] and [2]; Videos of the crew assembling truss in both the WETF and on orbit showed the reason: manipulating and actuating the joint was necessarily a two-part task in order to prevent accidental triggering of the joint; a "soft capture" allows the crewman to change his grip location from manipulation to actuation. However, we felt that the use of a clever assembly sequence, and the fact that our end effector had no need to let go and re-grip the joint, precluded the need for such a feature. This helped to simplify our designs even more.

Table 1: Robot-Friendly Structural Joint Design Requirements For ARASS

Requirement	Comments
Design loads: ± 1140 lb. axial ± 2620 in.-lb. bending	Based on early space station docking and crew tether loads.
Preload after tightening: 3000 lb	Good preloaded joint design practice.
Capture envelope: ± 0.10" linear ± 3.0° angular	Based on conservative estimate of accuracy of vision system.
Sideways insertion.	Required for strut replacement.
One arm fastening operation.	Only one arm available.
Joint must be clocked* & torsion countered via a positive mechanism (not friction alone).	Certain struts require a specific orientation that must be maintained throughout the life of the station.
Alignment guide should be provided as part of the end effector if possible.	Minimizes joint complexity, weight.
A "soft capture" device is uncessary.	Reduces complexity fo the joint. The robot never needs to let go of the strut so long as the end effector provides the necessary degrees of freedom to accomplish fastening.
Must make provision for vision system fiducials (reference makings) on joint & scar.	Vision system must have an alignment target which is visible from directly over the insertion point.
EVA backup operation.	A tool will probably be required.

Test Articles

Based on discussion and review of robotic truss assembly and its requirements, four joint design concepts were developed, each of which addressed the robotic alignment problem and the structural fastening task in a different way. These joints are pictured in figures 2 through 5, and their cross sections are shown in figure 6. For all joints, the half which is mounted to the node ball (the common attachment point at each corner of the truss) is referred to as the "scar," shown in figure 6-A. Detailed descriptions of each joint design are in Appendix A.

Fig. 2 Threaded Collar Joint

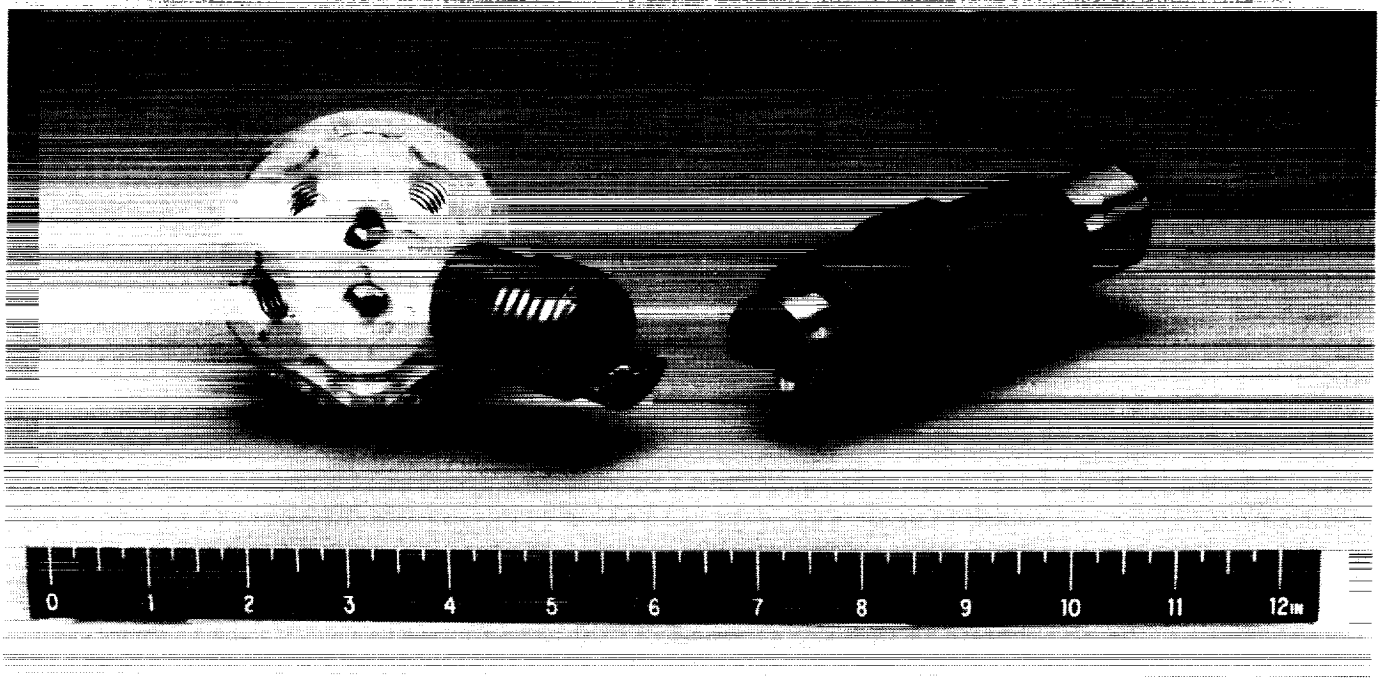

Fig. 3 Collet/Flex Drive Joint

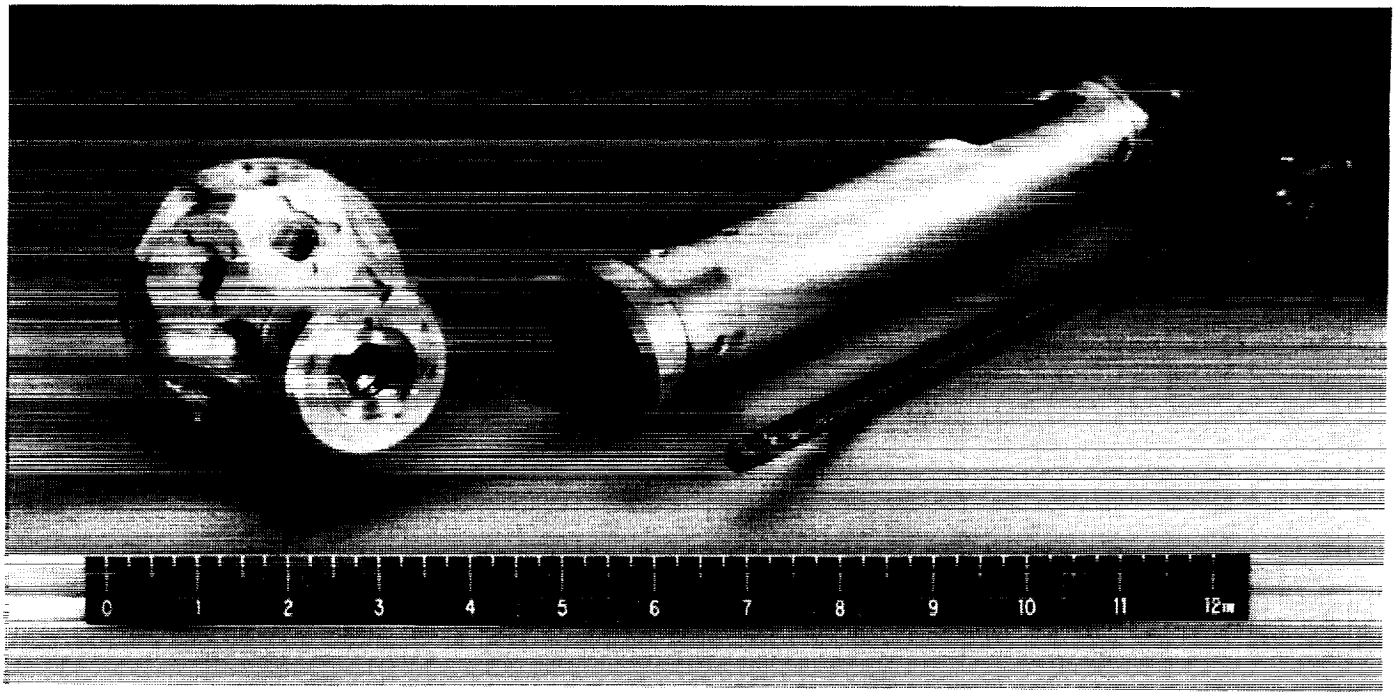

Fig. 4 Bolted/Flex Drive Joint

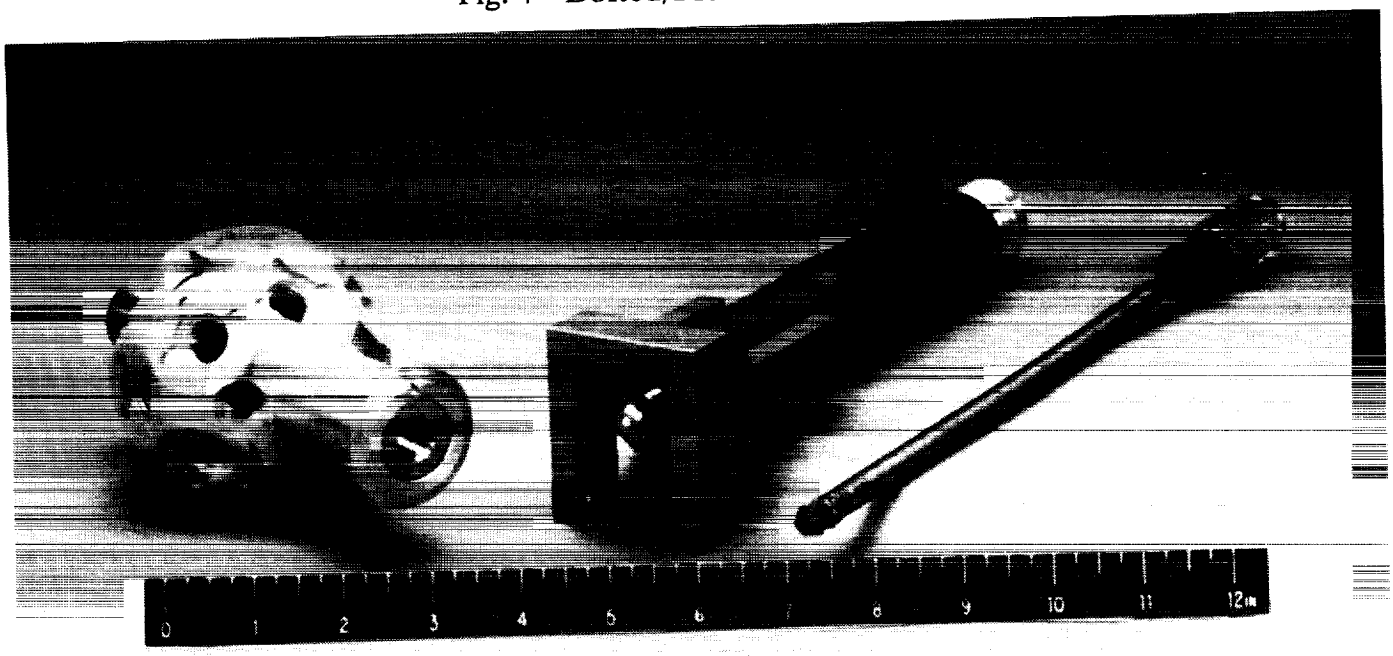

Fig. 5 Hammer-Head Joint

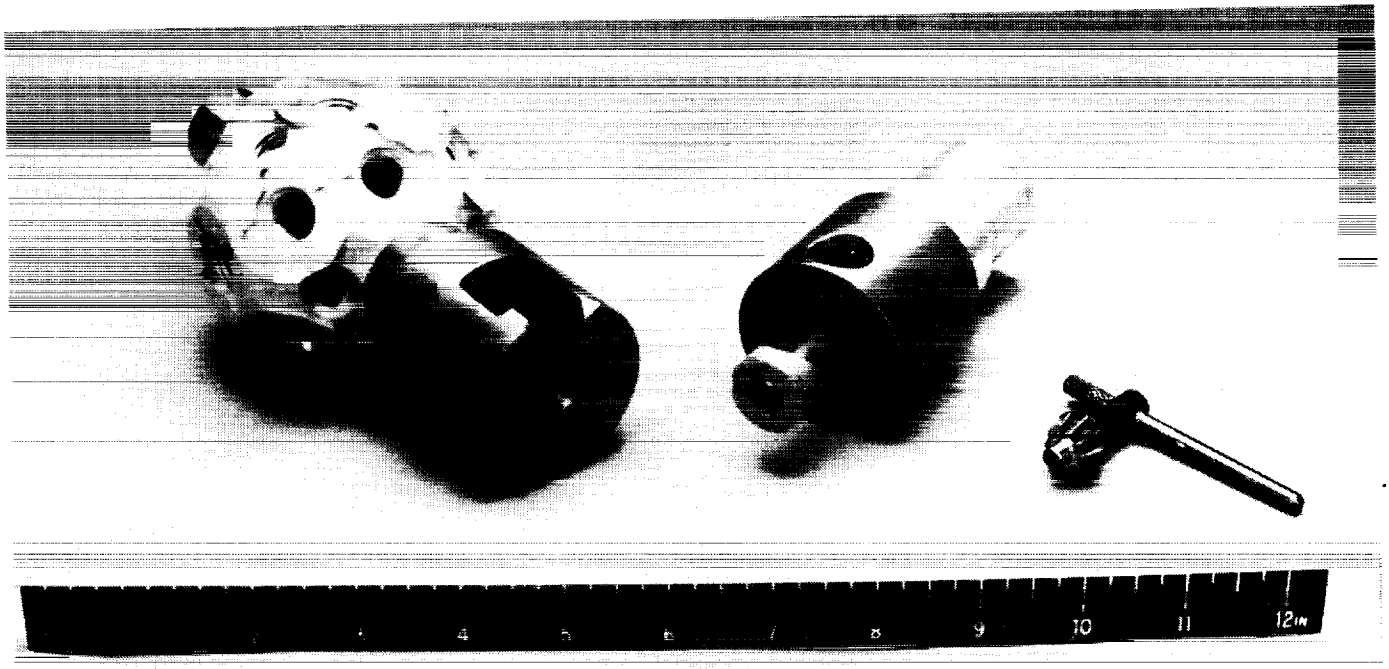

Fig. 6 Robot-Friendly Structural Fasteners Evaluated by the Robotics and Mechanical Systems Laboratory

a) THREADED COLLAR JOINT

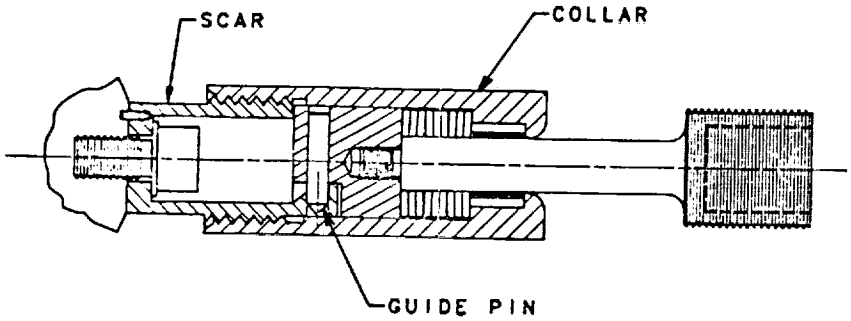

b) COLLET/FLEX DRIVE JOINT

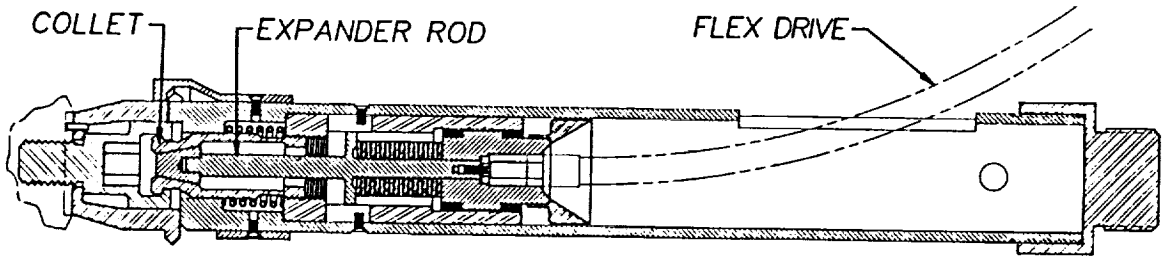

c) BOLTED/FLEX DRIVE JOINT

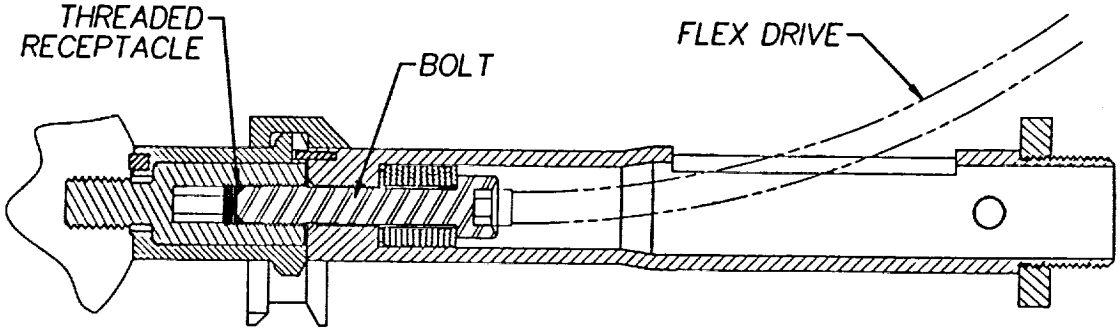

d) HAMMER-HEAD JOINT

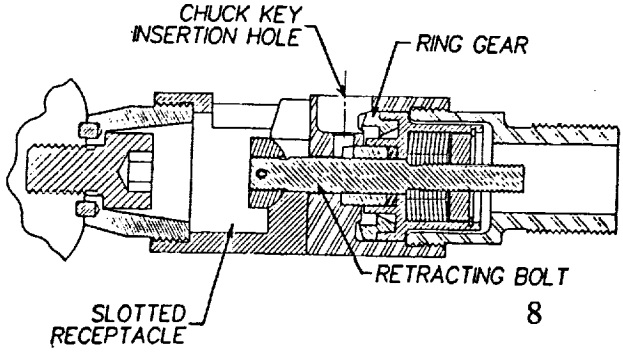

Testing

The four prototypes were manufactured, and each joint put through a series of identical tests, shown schematically in figure 7. The robot-friendliness tests used a robotic manipulator to quantify how well each joint went together under 1) linear and angular misalignments, 2) control of a computer vision system, and 3) linear and angular misalignments to a scar at the end of a flexible truss tube. Structural testing was performed using standard structural test equipment to quantify the joints' axial, bending, and torsional properties. A detailed description of all of these tests is in Appendix B.

Fig. 7 Robot-Friendly Joint Selection Process

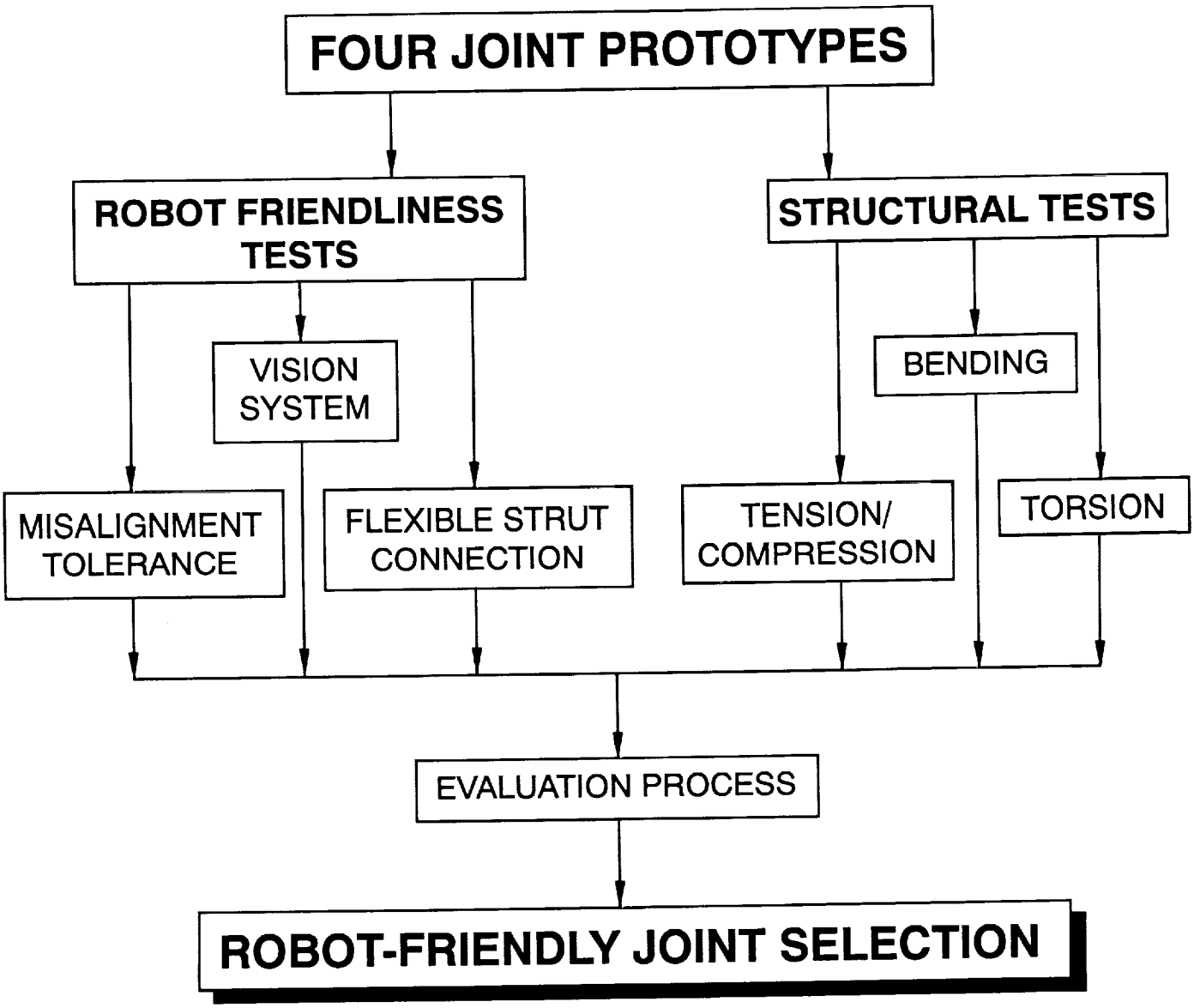

Results

All the joints met or exceeded the misalignment design requirements. Vision system testing revealed no major incompatibilities, nor were there any difficulties in making attachment to the flexible node simulator. All joints exhibited reasonable structural properties. The coordinate system referenced in the remaining discussions is shown in figure 8.

Fig. 8 Joint Coordinate System

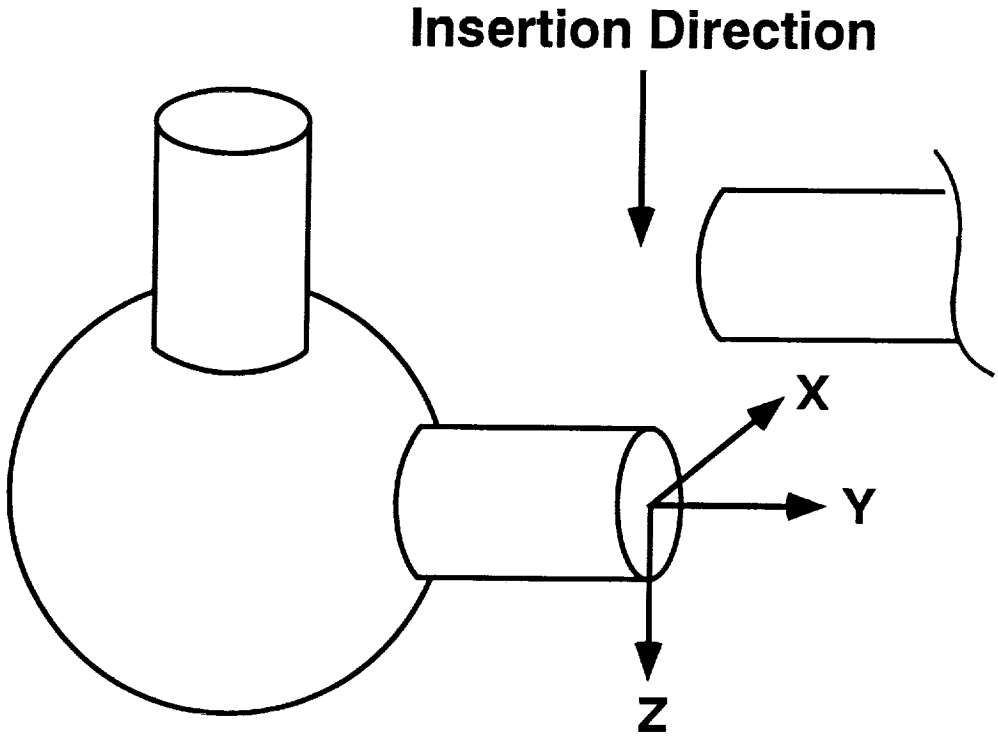

Robotic Testing Results

All the joints were able to capture under all the misalignment requirements. However, no joint could be *tightened* under every misalignment. Very high Z-forces developed as the capture guides forced the joints together during insertion. Tighter alignment guides (i.e., those which provided a closer fit with their scars) produced higher capture forces because they tried to correct the misalignment as the robot pushed the joint halves together. Higher actuation torques were usually required during the tightening process as the misalignments became more severe. Angular misalignments created the highest forces and moments (with roll about the Z-axis producing the highest of all) and all instances of "no connection possible" were caused by these misalignments. The two threaded joints were very intolerant of angular misalignments, but had no cross-threading problems otherwise.

The vision system performed very well. Our fiducials were a pair of cross hairs placed 25.4 mm (1 inch) apart on the scar. We were able to compensate for up to approximately 20 cm (8 inches) in depth and ±7° of roll. Tightening a joint which had been inserted under vision control never produced more than 44 N (10 lbs.) of residual Z-force.

There were no problems in connecting to the flexible node simulator. In fact, the compliance inherent in the simulator usually *helped* the joint to slide together under severe misalignments.

The following are some specific comments on each joint:

Threaded Collar: Although the guide pin worked well to align the joint for lateral misalignments, it tended to jam under severe angular misalignments. This could have been alleviated by greater chamfering of the guide pin hole and a hard surface finish on the pin (the prototype was made of unanodized 6061 aluminum). This joint was felt to have the best visual verification—both for tightening and for loosening—because of its highly visible external collar.

Collet/Flex Drive. The Collet/Flex Drive's capture guide gave it a very large X-direction misalignment tolerance. However, under some angular misalignment conditions, it appeared that the capture guide had pulled the joint together but the collet assembly could not be advanced into the receptacle. Also, sometimes the assembly would stick in its advanced position, making joint removal difficult. There were also some minor problems with vision system compatibility: the capture guide partially blocked the camera view and a special fiducial was required due to the tapered section of the scar (because the cross hair became distorted when taped to the surface of the conical section).

Bolted/Flex Drive. Like the previous joint, this one also had very large X-direction misalignment tolerance. But although the capture guide pulled the joint together well, and the tip of the bolt would start into the scar, it always jammed under roll-X and roll-Z misalignments. This joint also produced the highest moments about the Y-axis during roll about Y misalignments, indicating that it had the best clocking correction device (it is also worth noting that the joint always went together under this misalignment with only a slightly higher than normal tightening torque). The tangs of the alignment guide stuck well down below the joint (see figure 6-C) and partially blocked the corners of the camera view during vision system testing.

Hammer-Head. The Hammer-Head turned in the best performance in misalignment tolerance, jamming only once (on the most severe roll about Z misalignment). However, its clocking mechanism did not perform very well—the retracting bolt was free to rotate about the Y-axis enough that it was unable to tightly clock the joint. Its negative roll about X tolerance was outstanding (27°) due to the cylindrical shape of its head (about the X-axis). This joint also had the lowest capture forces. Its roomy capture guide permitted it to align very easily. The retraction of the head then removed all remaining misalignments and pulled it together nicely. As for vision system compatibility, the Hammer-Head itself extended slightly into the camera view, and the vision system was fooled once by the discontinuity where the two halves of the scar are screwed together (see figure 6-D). This was because the discontinuity appeared as a line to the camera (when viewed from the correct angle), and the vision system then mistook it for part of a cross-hair.

Structural Testing Results

The structural test data for the axial and bending tests were processed with specially written FORTRAN computer code. The data were then downloaded to Macintosh computers for plotting. Least-squares curve-fitting was applied to the data to extract stiffnesses.

The amount of out-of-plane bending in the axial tests turned out to be insignificant—never more than 0.3°. The 445 N (100 lbs.) load tests' data were very noisy and inconsistent. The best linearity and repeatability was achieved in the 8900 N (2000 lbs.) load range. Figure 9 shows load versus deflection curves for each of the four joints. These curves, as well as the values listed in the evaluation matrix (table 2, to be discussed in the next section), are for axial stiffness (K) in this load range. The stiffest joint was the Threaded Collar Joint, possibly due in part to its large collar area and the fact that its narrow shaft was constructed of a very stiff material, MP35N. The least stiff was the Collet/ Flex Drive, which showed indications of having lost some of its preload.

Fig. 9 Load Versus Deflection Curves for All Joints (± 8900 N Axial Load)

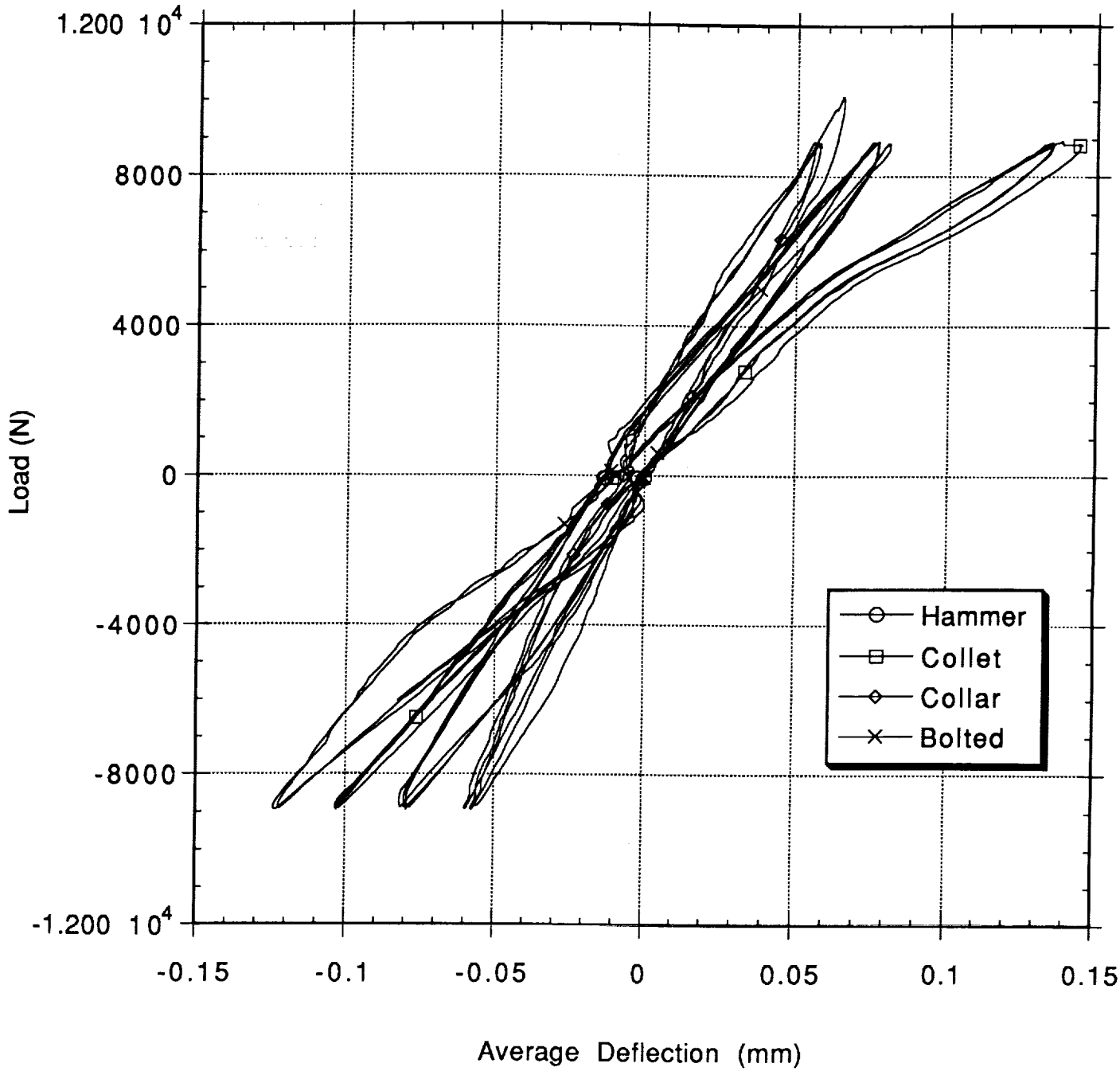

Fig. 10 Moment Versus Bending Deflection Curves for the Hammer-Head Joint, All Four Bending Planes (± 226 N-m Bending Moment)

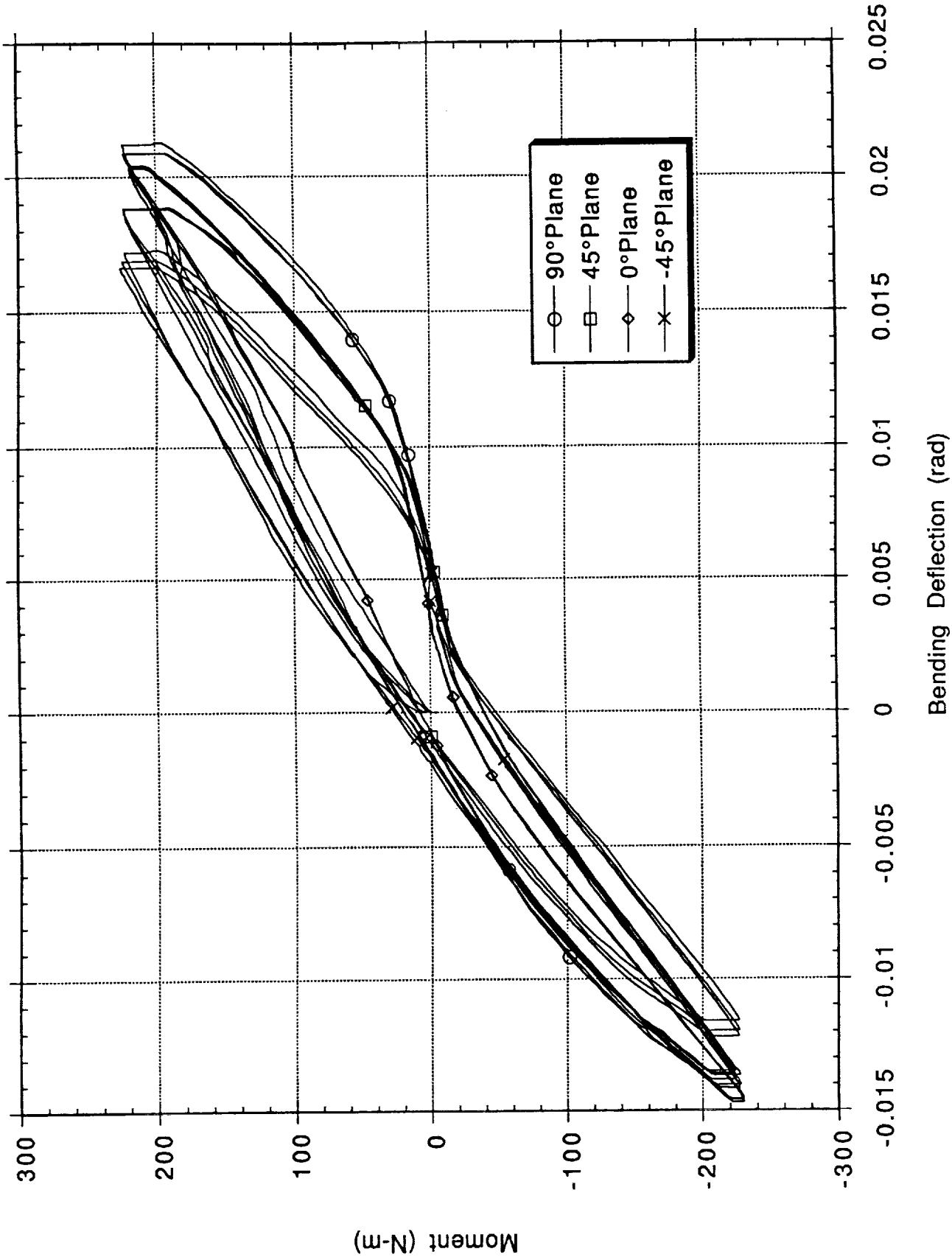

In the bending stiffness tests, the higher load case again gave more consistent values. The Threaded Collar and the Hammer-Head exhibited consistent stiffness in all bending planes, whereas the Bolted/Flex Drive and the Collet/Flex Drive showed considerable variance. (However, these variances do not appear to be related to each other in any way.) The Hammer-Head had the highest stiffness (12,900 N-m/rad, 114,000 in-lbs./rad), probably due to the fact that it had the largest (50.8 mm, 2 inches) diameter contact area. The Threaded Collar had the lowest stiffness (5800 N-m/rad, 51,400 in-lbs./rad), evidently due to its narrow section. Figure 10 shows typical moment versus bending deflection curves for one of the joints.

Although the figure of merit for axial loading—axial stiffness—was rather obvious, this was not so for bending. It seems that the most critical failure mode for this truss is in column buckling. Therefore, the figure of merit for bending is column end fixity. This is because a joint with a lower end fixity would require a thicker-walled, heavier truss tube in order to accommodate the same buckling load as a joint with a higher end fixity. Therefore, from a systems standpoint, end fixity becomes more important than bending stiffness [9]. Values for column end fixity (C) for both longeron and diagonal truss members were computed using the joint bending stiffnesses. The value of C was less for longerons because of their thinner wall, and it is these values which we chose to use for comparison (to be discussed in the next section). The values of C shown for each joint in table 2 were averaged over the four bending planes.

The torsional stiffness test data was very inconclusive. The deflections were in the noise range. However, they did reveal how much clocking "slop" or "play" each joint had when the load direction was reversed. The Hammer-head displayed the highest slop, almost 11°, while the next highest was only 1.2°.

Discussion

At the conclusion of the testing, the joint design and evaluation team used a weighted matrix evaluation scheme to determine the best overall fastener. The final matrix is given in table 2. Six criteria were deemed important to our structural assembly task:

1. *Reliability of fastening.* The figure of merit here was the number of times the joint could be connected out of the 20 misalignment cases in the first battery of misalignment tests.
2. *End effector simplicity and reliability.* The fewer degrees of freedom, the fewer complex motions, and the lower the technology risk of the end effector design, the higher the reliability score of the overall system. The end effector also scored higher if it did not need to provide an external capture guide for the joint. This score was assigned after group consensus.
3. *Structural performance.* There was considerable discussion as to whether axial stiffness or end fixity was the more important attribute. We eventually compromised and weighted them equally. All the joints were ranked according to their percentage of the highest K (for axial) and C (for bending); these two scores were then added, averaged, and normalized to result in the scores shown.
4. *Low cost to manufacture.* Cost is always an important consideration, especially when many hundreds of these joints might be manufactured. For these evaluations, the cost to build each prototype was used as the figure of merit.
5. *Visual verification.* This criterion was best evaluated by answers to some key questions: Could you see if the joint was tight, or verify that it was completely disengaged when trying to take it apart? Could the joint be visually inspected as part of regular space station maintenance to verify that it was fully tightened? This score was assigned after group consensus.
6. *Low weight.* Minimal weight is always important in space flight systems. It was assumed that the prototype weights would be indicative of the relative weights of each concept even after weight optimization. The weight of each prototype, which includes its scar, was used as the figure of merit.

Table 2 Robot-Friendly Structural Joint Evaluation Matrix

Criteria \ Joint		Bolted/Flex Drive			Collet/Flex Drive			Threaded Collar			Hammer Head		
Reliability of Fastening	WT 9.2	12 of 20 connections	SC 6	WT SC 55.2	13 of 20 connections	SC 7	WT SC 64.4	13 of 20 connections	SC 7	WT SC 64.4	19 of 20 connections	SC 10	WT SC 92.0
EE Simplicity/ Reliability	6.2	Complex cap. guide Flex drive actuator	3	18.6	Simple cap. guide Flex drive actuator	4	24.8	No capture guide Untested worm gear drive	6	37.2	No capture guide Simple drive	10	62.0
Structural Performance*	4.8	K=8.44 x 10E7 N/m C=2.01	8	38.4	K=6.94 x 10E7 N/m C=1.87	8	38.4	K=1.49 x 10E8 N/m C=1.65	10	48.0	K=1.09 x 10E8 N/m C=2.18	10	48.0
Low cost to Manufacture	4.2	Prototype cost: $4,800	9	37.8	Prototype cost: $9,200	5	21.0	Prototype cost: $4,200**	10	42.0	Prototype cost: $5,600	8	33.6
Visual Verification	3.0	Poor: Guide is in way, Cannot tell if bolt is retracted	2	6.0	Fair: Guide is not large, but still hard to see collet	6	18.0	Best: Easy to see how far collar has advanced	10	30.0	Good: Easy to see head	8	24.0
Low weight	2.6	881 g (1.94 lb)	9	23.4	1409 g (3.11 lb)	5	13.0	898 g (1.99 lb)	9	23.4	782 g (1.72lb)	10	26.0
Total weighted score	30			179.4			179.6			245.0			285.6

* K = axial stiffness, C = column end fixity

** Evaluation team estimate

The team voted on what weighting to assign each of the six criteria with a requirement that the weights must add up to 30 (allowing a possible 5 for each criterion). The team then considered each criterion, as discussed above, and assigned scores for each joint. The best joint for each criterion was always assigned a score of "10" and the others ranked relative to it. The score times that criterion's weighting resulted in a weighted score, and the weighted scores were then added for the final total. Note that in this type of evaluation, the top score must be at least 10% higher than the runner-up to produce conclusive results. The highest scoring joint was the Hammer-Head, scoring 285.6 out of a possible 300 points.

DFA Recommendations

We learned a lot about designing for robotic assembly in the course of the study. First of all, designing so that chamfers slide on chamfers always produces smoother assembly than corners working against chamfers. Corners are much more likely to dig into the chamfer and jam. Second, a chamfer sliding on a cylindrical surface works amazingly well. This was demonstrated by the Collet/Flex Drive's and Bolted/Flex Drive's capture guides against their large cylindrical scars. The Hammer-Head also had many of these types of surfaces—two cylinders on the head and one on the retracting bolt shaft—which worked well against both chamfers *and* corners. Furthermore, sliding surfaces must have a hard surface finish or they will gall upon each other. Good sliding surfaces may be created by calling out smoother surface finishes (e.g., 63 RMS or finer), or by surface treatments such as hard anodize (on aluminum) or dry film lubrication.

We found the best clocking alignment device to be a dowel pin moving downward into a chamfered slot, as used in the Bolted/Flex Drive (illustrated in figure 11). Notice that it embodies the concept of cylinder-on-chamfer as well.

Fig. 11 Cross Section of Pin-in-Slot Clocking Device Used On Bolted/Flex Drive Joint

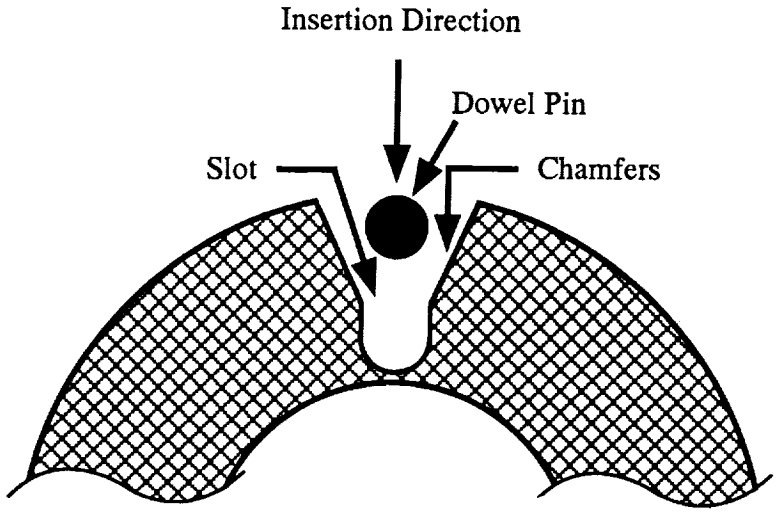

Finally, it is a good idea not to try complete final alignment while inserting, as was demonstrated by the Hammer-Head. Tighter alignment guides try to do too much at once, and wind up jamming the connector before the actuator has a chance to tighten it. The Hammer-Head, for instance, does not try to seat the joint until the motor drive is retracting the head—and 13,300 N (3000 lbs.) of alignment force is available to pull the head into its seat.

"Real World" Robotic Observations

There are many problems which will never be identified by studying the perfect world of computer graphics models. These can only be flushed out by tests with real hardware. The following are some observations made during the course of this testing:

Force/torque sensor data must be interpreted carefully. The force/torque sensor data from the first battery of robotic misalignment tests had been plotted using bar graphs to better analyze overall trends. What we noticed after looking at the plots was that if you put the linear misalignment in X data plots next to the roll misalignment about Y plots, it was difficult to tell which was which. The same held true for linear misalignment in Y and roll misalignment about X. Evidently, the reaction of the capture guide to an X-misalignment is a force which induces a torque about the Y-axis. Thus, the reaction looks like that of a roll about Y. Similarly, the guide's reaction to a Y-misalignment is an induced torque about the X-axis, and that is why these two plots look so similar. The significance of this result is that given *one* set of data from a force/torque sensor, you cannot absolutely determine what type of misalignment condition you are faced with. Some supplemental data from other sensors, or perhaps even some diagnostic test movement, must be applied in order to make the assembly operation more robust (this diagnostic testing could be an application for artificial intelligence or a neural network).

Real robots aren't rigid. For instance, the robot used in our testing complied 2.5 mm (0.1 inch) under a 67 N (15 lbs.) load (in one direction). This compliance is dependent upon the configuration of the arm and the direction in which the load is applied.

Real robots sag under gravity. Never believe the position and orientation quoted by your robot control computer. Our measurements showed that a supposedly level gripper was actually angled by about 1°. This is why we always tried to use external measurements when setting up our offsets for misalignment testing. This same sag also makes it difficult to confirm a tool offset because the robot's sag changes as the manipulator's configuration changes—the manipulator *wants* to rotate about the correct toolpoint, but it *physically cannot.* The robot's sag under gravity also caused the linear in X misalignment data to be biased toward the robot; i.e., the robot was more compliant in the +X direction because it was sagging in the -X direction. This phenomenon might not occur in the microgravity environment of low Earth orbit, but larger, crane-type manipulators handling large payloads might see a similar effect due to orbital mechanics.

Real robots are machines—they experience hysteresis, thermal expansion, and friction. We saw sluggish response when reversing direction, and mechanical drift when making orthogonal changes in direction. We only noticed these effects because we were taking measurements to the 1/40th of a millimeter (thousandth of an inch), and these effects were on the order of 0.5 mm (0.02 inch). For this same reason, we had to "exercise" the robot every morning for about 45 minutes before testing. The robot, being all aluminum, would "grow" some 0.5 mm (0.02 inch) or so as it warmed up. We also noted that this warm-up changed the friction at the joints, and that affected the drift and hysteresis of the system. Again, all of these effects were arm-configuration dependent.

Conclusions

This study has shown that a structural fastener can be designed via the application of DFA principles so that it is both easily and reliably connected by a robot manipulator operating under automated control. This fastener also exhibits good structural properties. Previous research has shown that such a design will be easier to assemble by humans as well. With this in mind, we recommend that such methodologies be applied *now* to future space system designs to ensure maximum flexibility of operation by both humans *and* robots.

Appendix A

Design Descriptions of the Four Robot-Friendly Structural Fasteners

This appendix contains detailed descriptions of each of the four "robot-friendly" structural fasteners evaluated for this study. Reference is made to figures 2 through 6, which are to be found in the main text.

First, one will notice a feature common to all of these designs: each incorporates belleville spring washers. In all cases, this stack of bellevilles is deflected at the end of the joint tightening process and thus transmits a preload to the joint interface.

There is a very good reason for the use of belleville washers here. Observe that the connection is being made along the axis of a tube. When tightening these connectors, the moment arm available (i.e., the radius of the strut) for straightening out the tube is extremely short (about 25.4 mm, or one inch), whereas any sideways resistance forces along the tube have the entire length of the tube for a moment arm. Viz, in the laboratory, we bolted and preloaded (without any bellevilles) a vertically oriented 5-meter truss tube at one end, then let go of it. The tube then righted itself, and the joint completely loosened! The best way to prevent this phenomenon from occurring was to include belleville washers which build up their preload over many thousandths of an inch of deflection. Thus, when the truss tube righted itself after being released, the "relaxation" of a few thousandths of an inch would only minimally reduce the preload.

A noteworthy side benefit of this belleville arrangement is that the motor which is applying the preload torque now ramps up to the full preload torque value over a longer time period. This is much better for the life of the joint tightener's drive train. Descriptions of each joint now follow.

Threaded Collar Joint. The Threaded Collar joint is shown in figures 2 and 6-A. The principle feature of this joint is that it reduces the insertion problem to that of the well-studied pin-in-hole task. The pin and the scar's guide pin hole both have chamfers to facilitate the insertion process. The scar has an external thread, and the collar a matching internal thread. Ultimately, the collar would also have an externally cut gear profile which would be engaged by a worm gear on the end effector. This would provide the collar rotation.

Initially, the collar is held retracted by a light compression spring force such that the guide pin is fully exposed (as shown in figure 2). As the two joint halves slide together, the guide pin is inserted into the guide pin hole on the scar and accomplishes clocking of the joint. Then the collar is slid to the left (as viewed in figure 6-A) and simultaneously rotated by the worm gear to engage the threads. It is theoretically possible for the worm gear alone to accomplish both motions; i.e., the worm's rotation would slide the collar to the left until it met resistance, then force the collar to rotate and thread onto the scar.

Collet/Flex Drive Joint. The Collet/Flex Drive joint is shown in figures 3 and 6-B. This design is essentially a robot-compatible version of a previously developed EVA design (see "JSC Truss Joints" in [4]). Its principle of operation involves an expander rod which forces a set of collet fingers to expand outward into a receptacle to achieve connection. End effector drive engagement is accomplished by using a section of commercially available flexible drive shafting with an allen head wrench welded to the end. The hand-operated version of this tool is shown to the right of the joint in figure 3.

Before connection, the entire collet assembly is held inside the joint body by a light compression spring force. The joint halves are slid together with the assistance of a two-fingered external guide. Clocking is performed by a wedge

protruding from the joint face which engages a matching receptacle on the scar as the two halves are slid together (these are visible at the top of the joint interface surfaces in figure 3). Then the flex drive is inserted into a slot in the joint body. The tip of the allen head wrench simply slides along the inside wall of the body, up a conical ramp, and into a matching hex hole in the end of the collet assembly. Continued axial pressure by the flex drive overcomes the compression spring force, and pushes the collet assembly out of the joint body and the collet fingers are extended into the receptacle. Rotating the flex drive at this point begins to advance the expander rod so that it forces the collet fingers outward. Note that this joint needed the lowest input torque to achieve a 13,300 N (3000 lbs.) preload as a result of the collet's wedging action combined with its threaded actuation.

Bolted/Flex Drive Joint. The Bolted/Flex Drive joint is shown in figures 4 and 6-C. This joint is probably the simplest possible—save for its capture guide. It is a basic, bolted joint which incorporates the same flex drive system as the previous design. The bolt is a modified, standard socket head cap screw: its tip has been heavily chamfered, 3/4 of a diameter's worth of threads near the tip have been removed, one diameter's worth of threads retained beyond that, and then the remaining threads from there to the head removed as well. Both the joint body and the receptacle are threaded.

Initially, the bolt is completely retracted into the body. The two halves of the joint are slid together with the help of an external guide. Clocking is achieved via a pin on the joint side which slides into a narrowing, wedge-shaped slot on the scar (the slot is visible on the front of the scar in figure 4). The flex drive is inserted, begins to rotate, and engages the bolt. As the bolt advances, its tip brings the two halves into proper alignment before the threaded portion begins to engage the receptacle. By the time the bolt head begins to compress the bellevilles, the threaded portion of the bolt is engaged only in the threads of the receptacle, and the interface can be properly preloaded.

Hammer-Head Joint. The Hammer-Head joint is shown in figures 5 and 6-D. It operates on the principle of inserting a cylindrical head into a wide, well-chamfered hole, then using the joint's actuation to achieve final alignment as it is tightened. A standard chuck key is inserted through a hole in the side of the joint, engaging a ring gear. When the key is turned, the ring gear turns a nut which then retracts the bolt. It is essentially a bolted joint; however, it has eliminated the possibility of cross-threading by turning a nut whose threads are always engaged with the bolt.

Hammer-Head operation starts with the head extended as shown in figure 5. The capture guide is essentially incorporated into both halves of the joint. As the two halves of the joint slide together, clocking is accomplished by flats on either side of the retracting bolt conforming to the flat sides of the slotted receptacle. The chuck key is inserted, turns the ring gear and nut, and the joint is drawn into alignment as the transverse cylindrical head seats itself in the mating receptacle.

Appendix B
Test Procedures Used in the Robot-Friendly Structural Joint Study

This appendix gives a detailed description of the test battery illustrated in figure 7 of the main text. The coordinate system referenced is repeated for convenience in figure B-1.

Fig. B-1 Joint Coordinate System

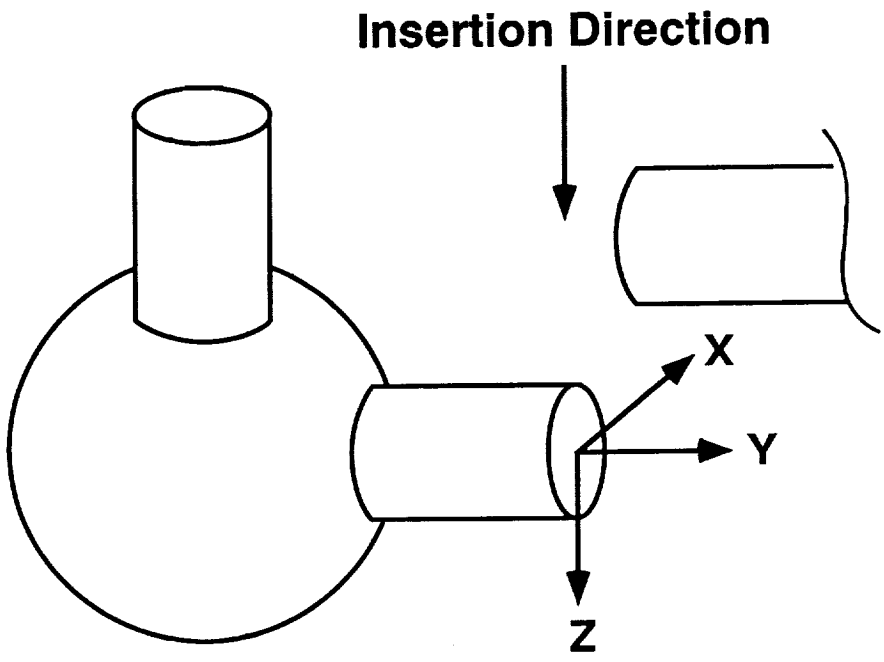

Robot Friendliness Tests

All robot tests were performed in the RAMS lab using a Robotics Research K-1607 seven degree-of-freedom manipulator. A commercial JR3 force/torque sensor was used to measure the forces and torques at the joint interface. The testing was performed in three phases.

Phase I. The first phase of the testing was designed to quantify the misalignment tolerance of each joint. We felt this to be the most important measure of "robot-friendliness". A node ball with the appropriate scar attached was mounted rigidly to the floor in front of the robot. Thirty-two misalignment measurements were made.

The first battery of misalignment tests was aimed at determining how well each joint met the design requirements. These first tested each joint at one-half of its requirement (± 1.27 mm or .05 inch for linear and ±1.5° for angular) and then at the full requirement (±2.54 mm or 1 inch and ±3°). These four measurements were made for each of the following five misalignment conditions: (1) linear in X, (2) linear in Y, (3) roll about X, (4) roll about Y, or clocking, and (5) roll about Z. In each case, the joint was held by the robot approximately 51 mm (two inches) above the insertion

point. The misalignment was input in hand coordinates using the robot's teach pendent as measured by an external device. The joint was inserted, tightened, and the maximum forces (induced by these operations) recorded for later analysis. The test was stopped and "no connection possible" declared if the Z-direction insertion force exceeded 90 N (20 lbs.).

The second battery of misalignment tests was meant to determine the maximum misalignment each design was capable of tolerating. Each of the five conditions above was tested again, but with larger and larger misalignments until the capture guide no longer pulled the joint together. In addition, two Z-direction tests were added: could the joint pull itself together and be tightened (1) with a 90 N (20 lbs.) overload, and (2) when the joint had not been inserted all the way.

Phase II. Vision system compatibility was the second phase of robot-friendliness tests. These tests were intended to determine if there were any incompatibilities between the joint and the planned vision system alignment and insertion scheme. These might be in the form of camera view blockage, features on the scar which might confuse the vision system, etc. In addition, we wanted to know if there were any residual misalignments after vision system-controlled insertion which would inhibit proper fastening.

Fig. B-2 View of General Test Setup

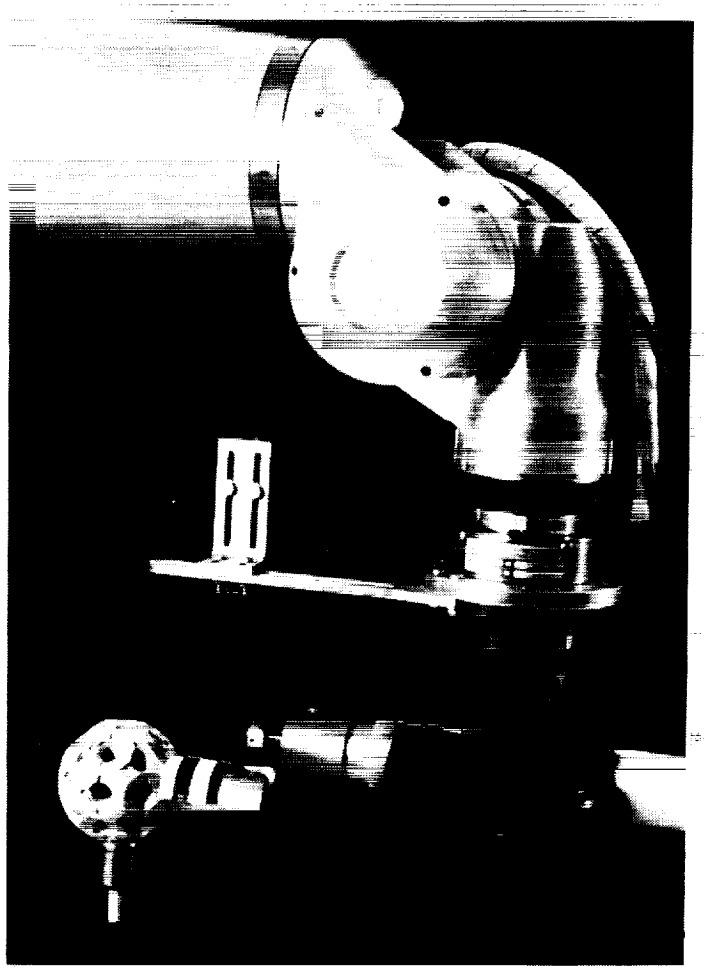

Visible are the robot, force/torque sensor, vision system camera, truss joint, scar, and node ball atop the flexible node simulator (see text).

The vision system camera was located on the end effector just beyond the end of the joint as shown in figure B-2. A fiducial, or reference mark, was placed on the joint's scar such that when the joint was properly aligned, the camera was centered over the fiducial. At the start of the test, the robot needed only to be positioned so that the fiducial was within the camera's view. The vision system then commanded the robot in X, Y, Z, and roll about Z until the joint was positioned 63.5 mm (2.5 inches) directly above the insertion point. The robot then moved forward 63.5 mm (2.5 inches) in Z to make the insertion.

Five different initial misalignments were used in the testing. These five points are depicted graphically in figure B-3. For instance, point 1 was at a location +X, +Y and -Z from what would be the perfect alignment point (i.e., 63.5 mm or 2-1/2 inches above the actual insertion point). Point 2 added a roll misalignment to that, and the remaining points tested other combinations of X, Y, Z, and roll misalignment (including having the joint too close). Residual forces and torques were recorded immediately after insertion and then again after the joint was tightened.

Fig. B-3 Location of Vision System Test Points
(as seen from the end effector camera)

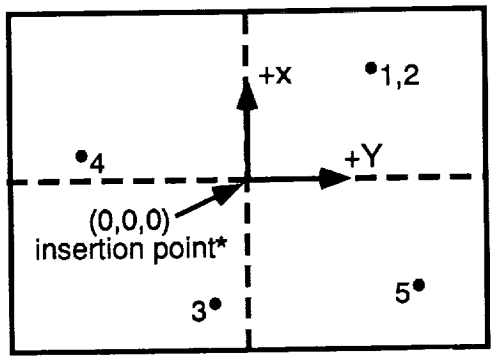

Phase III. We predicted that the most difficult joint connection necessary in assembling the 5-meter truss was going to be that to a node which was at the top of a vertical truss member anchored only at its bottom end (this situation is depicted for the robot on the right in figure 1 in the main text). A simulation of this particular task was constructed by attaching a node ball with some additional mass to the end of a steel rod which was then anchored to the floor in front of the robot as shown in figure B-2 (Note: additional mass is not shown). The stiffness of the rod and the additional masses were chosen such that the simulator mimicked the stiffness and frequency of vibration of an actual 5-meter strut with a node ball attached. The third phase of robot-friendliness tests was performed with this flexible node simulator. Both of the previously described maximum misalignment and vision system tests were repeated.

Structural Tests

The purpose of the structural test program was to gather data to be used to compare the joints in structural stiffness, linearity, and repeatability. The tests were conducted in the Structures Test Laboratory at JSC. Details of these tests may be found in the structural test plan [10].

Axial stiffness tests were run first. Each joint was mounted in an Instron test machine with one linear voltage differential transformer (LVDT), attached at every 120° around its periphery. Together, the three LVDT's would

measure the relative displacements between the planes of each joint half and therefore any out-of-plane bending induced by the tensile or compressive load. Their average would constitute the total joint deflection. Each joint was preloaded to 13,300 N (3000 lbs.) before testing. The loads applied were ±445, ±4450, and 8900 N (±100, ±1000, and ±2000 lbs.). Loads were cycled three times for each load case, and data continuously recorded by a data acquisition computer.

Bending tests were run next. A pure couple was applied at the right end (as viewed in figure 6 of the main text) of each joint using a pair of opposed hydraulic actuators. Again, LVDT's were used to record the actual deflections along each of the 3 axes. The joints were again cycled three times to ±56, and ±226 N-m (±500, and ±2000 in-lbs.). These load cases were repeated in four different joint orientations (every 45° about the Y-axis) to look for any variances in bending dependent upon the joint's orientation. Again, data were recorded continuously.

The third set of structural tests examined torsional stiffness. Since relatively little torsional loading was expected for this space station truss configuration, the torsional data were only collected for completeness. Continuous data collection was not deemed necessary. Dead weights and pulleys were used to apply the load in five increments to a maximum of 27 N-m (240 in-lbs.). The loads were cycled three times—first clockwise, then counter-clockwise. The torsional deflection was measured by a string extensometer and recorded by hand at each load increment.

References

[1] Walter L. Heard Jr., Harold G. Bush, Judith J. Watson, Sherwood C. Spring, and Jerry L. Ross, "Astronaut/EVA Construction of Space Station," *AIAA SDM Issues of Intl. Space Station Conf.*, Williamsburg, VA., April 21-22, 1988. AIAA paper No. 88-2459.

[2] L. C. Thomas, "Space Station Truss Assembly Simulation and Fixture Evaluation (Second Series) Final Test Report," Feb. 9, 1988. JSC-32057.

[3] L. C. Thomas and L. P. Matranga, "Space Station LaRC Fixture Truss Assembly Simulation (Third Series) Final Test Report Phase 1 - Fixture Evaluation," May 17, 1988. JSC-32070.

[4] L. Thomas and L. Matranga, "Space Station Utility System Integration Phase II - Integrated Truss and Component Evaluation Final Test Report," June 7, 1989. JSC pub. #32088.

[5] Philip L. Sheridan, "Telerobotic Truss Assembly," *Proc. from the First Annual Workshop on Space Operations Automation and Robotics (SOAR '87)*, NASA CP-2491, pp. 487-491, 1987.

[6] Marvin D. Rhodes, Ralph W. Will, and Marion A. Wise, " A Telerobotic System for Automated Assembly of Large Space Structures," March 1989. NASA TM-101518.

[7] A. J. Scarr, D. H. Jackson and R. S. McMaster, "Product Design for Robotic and Automated Assembly," *Proc. from the IEEE Intl. Conf. on Robotics and Automation*, vol. 2, pp. 796-802, April 7-10, 1986.

[8] G. Boothroyd, "Effects of Assembly Automation on Product Design," *CIRP Annals: Manufacturing Technology*, vol. 32, no. 2, p. 511, 1983.

[9] J. E. Keever, "Final Report, Erectable Joint Trade Study," McDonnell Douglas report 2ITA409, May 14, 1990.

[10] George F. Parma, "Space Station Truss Robot-Friendly Structural Joints Structural Test Plan," March 26, 1990.

REPORT DOCUMENTATION PAGE

Form Approved
OMB No. 0704-0188

1. AGENCY USE ONLY *(Leave blank)*	2. REPORT DATE	3. REPORT TYPE AND DATES COVERED
	July 1992	technical paper

4. TITLE AND SUBTITLE
Development of a Truss Joint for Robotic Assembly of Space Structures

5. FUNDING NUMBERS
472-46-07-17

6. AUTHOR(S)
George F. Parma

7. PERFORMING ORGANIZATION NAME(S) AND ADDRESS(ES)
Lyndon B. Johnson Space Center
Structures and Mechanics Division
Houston, TX 77058

8. PERFORMING ORGANIZATION REPORT NUMBER
S-763

9. SPONSORING / MONITORING AGENCY NAME(S) AND ADDRESS(ES)
National Aeronautics and Space Administration
Washington, D. C. 20546-001

10. SPONSORING / MONITORING AGENCY REPORT NUMBER
NASA TP-3214

11. SUPPLEMENTARY NOTES

12a. DISTRIBUTION / AVAILABILITY STATEMENT
Unclassified—Unlimited
Subject Category 39

12b. DISTRIBUTION CODE

13. ABSTRACT *(Maximum 200 words)*

This report presents the results of a detailed study of mechanical fasteners which were designed to facilitate robotic assembly of structures. Design requirements for robotic structural assembly were developed, taking into account structural properties and overall system design, and four candidate fasteners were designed to meet them. These fasteners were built and evaluated in the laboratory, and the Hammer-Head joint was chosen as superior overall. It had a high reliability of fastening under misalignments of 2.54 mm (0.1 in) and 3°, the highest end fixity (2.18), the simplest end effector, an integral capture guide, good visual verification, and the lightest weight (782 g, 1.72 lb). The study found that a good design should incorporate chamfers sliding on chamfers, cylinders sliding on chamfers, and hard surface finishes on sliding surfaces. The study also comments on robot flexibility, sag, hysteresis, thermal expansion, and friction which were observed during the testing.

14. SUBJECT TERMS
Space Erectable Structures, Robotic Assembly, Joints (Junctions), Trusses, Orbital Assembly, Structural Design, Design for Assembly

15. NUMBER OF PAGES
32

16. PRICE CODE
A03

17. SECURITY CLASSIFICATION OF REPORT	18. SECURITY CLASSIFICATION OF THIS PAGE	19. SECURITY CLASSIFICATION OF ABSTRACT	20. LIMITATION OF ABSTRACT
Unclassified	Unclassified	Unclassified	Unlimited